Applied Geochemistry 24 (2009) 733–745

Contents lists available at ScienceDirect

Applied Geochemistry

journal homepage: www.elsevier.com/locate/apgeochem

Rare earth element composition of Paleogene vertebrate fossils from Toadstool Geologic Park, Nebraska, USA

D.E. Grandstaff *, D.O. Terry Jr.

Department of Earth and Environmental Science, Temple University, Philadelphia, PA 19122, USA

ARTICLE INFO

Article history:
Available online 25 December 2008

ABSTRACT

Fossil bones and teeth from terrestrial environments encode unique rare earth and trace element (REE and TE) signatures as a function of redox conditions, pH, concentrations of complexing ligands, and water-colloid interactions. This signature is set early in the fossilization process and serves as a paleoenvironmental and paleoclimatic proxy. These signatures can also be used to interpret temporal and spatial averaging within vertebrate accumulations, and can help relocate displaced fossil bones back into stratigraphic context. Rare earth elements in vertebrate fossils from upper Eocene and Oligocene strata of Toadstool Geologic Park, northwestern Nebraska, record mixing and evolution of Paleogene vadose or groundwaters and variations in paleoenvironments. REE signatures indicate that HREE-enriched alkaline groundwater reacted with LREE- and MREE-enriched sediments to produce 3-component mixtures. REE signatures become increasingly LREE- and MREE-enriched toward the top of the studied section as the paleoenvironment became cooler and drier, suggesting that REE signatures may be climate proxies. Time series analysis suggests that REE ratios are influenced by cycles of ca. 1050, 800, 570, 440, and 225 ka, similar to some previously determined Milankovitch astronomical and climate periodicities.

1. Introduction

Following the early Eocene thermal maximum, at about 55 Ma (Miller et al., 1987), global climates cooled from the Greenhouse climate of the late Mesozoic and early Paleogene to the Icehouse climate of the late Paleogene (Fischer, 1982). Marine records of this transition are marked by dramatic shifts in C and O isotopes near the Eocene–Oligocene boundary, the extinction of certain microfossil lineages, and the appearance of permanent glacial conditions on Antarctica (Ivany et al., 2003).

The Eocene–Oligocene White River Group (WRG) in NW Nebraska and SW South Dakota (Fig. 1) is a succession of nonmarine strata that records the final phases of this transition. Within the WRG, this transition is recorded by changes in sedimentation style (Evanoff et al., 1992; Terry, 1998), paleosol type (Retallack, 1983; Terry, 2001), and the extinction of various vertebrate and invertebrate lineages (Hutchinson, 1992; Evanoff, 1990). Although the overall trend during this transition is a change to progressively drier conditions in this region, the Eocene–Oligocene boundary is characterized by a dramatic decrease in paleotemperatures, but a negligible increase in aridity (Zanazzi et al., 2007).

The WRG also preserves one of the richest accumulations of vertebrate remains in the world, representing faunal assemblages from the Chadronian, Orellan, Whitneyan and Arikareean North American Land Mammal Ages (Prothero, 1996; Prothero and Whittlesey, 1998). Fossil assemblages have been recovered from all depositional environments throughout the entire section. Specimens range from isolated to fully articulated individual specimens in various environments, to mass death watering hole environments that preserve a combination of species in various states of articulation (Terry, 1996; Terry and Spence, 1997; Factor and Terry, 2002; Metzger et al., 2004; Mintz et al., 2005).

Signatures of lanthanide or rare earth elements (REE) in vertebrate fossils have been used to distinguish paleoenvironments (e.g., Wright et al., 1987; Trueman, 1999; Metzger et al., 2004; Patrick et al., 2004; Martin et al., 2005; Anderson et al., 2007) and to determine the taphonomy and provenance of fossil remains (Trueman and Benton, 1997; Staron et al., 2001; Trueman et al., 2003, 2005, 2006; MacFadden et al., 2007; Suarez et al., 2007b; Patrick et al., 2007). The abundant vertebrate remains from the WRG present an excellent opportunity to test the concepts of REE accumulation in nonmarine vertebrate materials as a function of changing paleoclimate, ancient depositional environments, ancient soil environments (pedogenesis), taphonomy, reworking and burial diagenesis.

This study investigates REE signatures in vertebrate fossils from the WRG at Toadstool Geologic Park (TGP), northwestern Nebraska, USA (Fig. 1). This study was undertaken to investigate how REE signatures in vertebrate fossils were influenced by changes in paleoenvironment and paleoclimate during this critical climate shift and to delineate the sources of REE incorporated in the fossils. The

* Corresponding author. Fax: +1 215 204 3496.
E-mail address: grand@temple.edu (D.E. Grandstaff).

0883-2927/$ - see front matter © 2008 Elsevier Ltd. All rights reserved.
doi:10.1016/j.apgeochem.2008.12.027

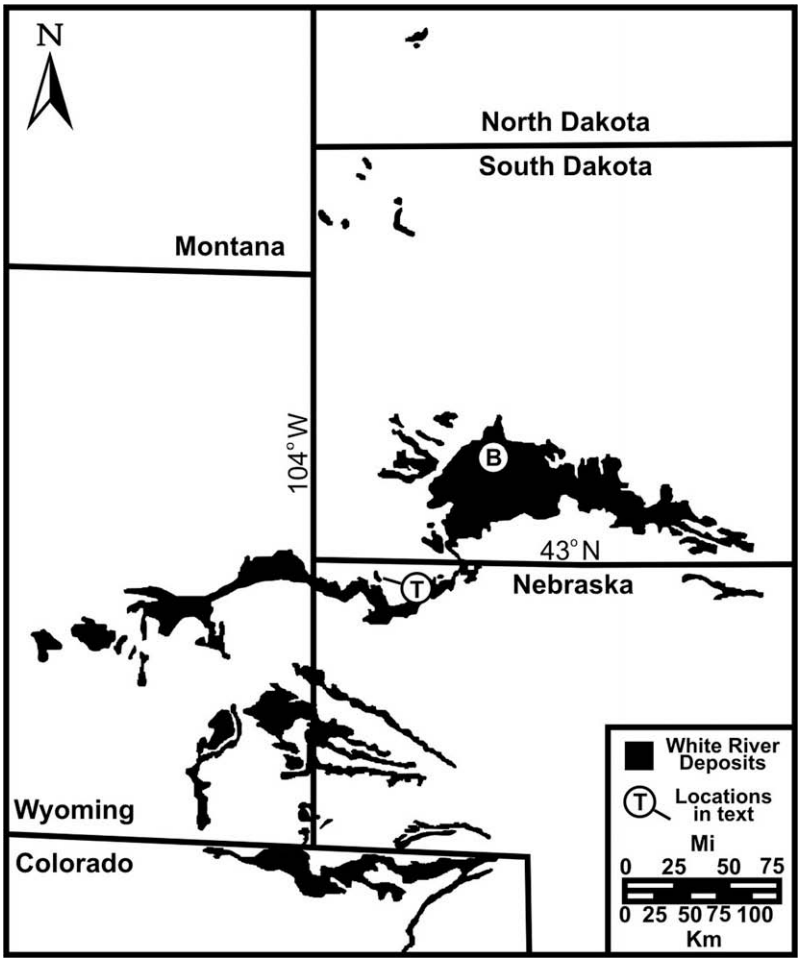

Fig. 1. Exposures of the White River Group across the northern Great Plains. T = Toadstool Geologic Park, Nebraska, B = Badlands National Park, South Dakota. Modified from Terry (2001).

variety of fossils analyzed also allows investigation of possible effects of taphonomy on REE signatures. Results from the TGP are compared with those from correlative strata of Badlands National Park (BNP), South Dakota (Metzger et al., 2004), approximately 150 km to the NE (Fig. 1).

2. Field area

Toadstool Geologic Park, administered by the US Forest Service, is located approximately 24 km NW of Crawford, Nebraska. A detailed locality map for TGP may be found in Terry (2001). The geologic framework used for this study follows that of Terry (1998, 2001), Terry and LaGarry (1998) and LaGarry (1998). Geochronologic control is based primarily on magnetostratigraphy (Prothero, 1996), but is supplemented with tephrostratigraphic correlations and associated age dates (Larson and Evanoff, 1998), and estimated rates of sedimentation (Zanazzi et al., 2007). Recognized depositional environments include fluvial, lacustrine and eolian settings that incorporate a mixture of clastic sediments derived from sedimentary, igneous and metamorphic rocks of various nearby Laramide uplifts (e.g., Black Hills uplift), rhyolitic and rhyodacitic volcaniclastics and airfall tuffs, and springfed tufa deposits (Clark, 1975; Larson and Evanoff, 1998; Terry, 1998; Evans and Welzenbach, 1998; Meehan, 1994). Overall, volcaniclastic sediments become more abundant up section.

The WRG in this locality rests unconformably on the Maastrichtian Pierre Shale. The unconformity represents a 30 Ma period of erosion and pedogenic modification throughout the region. It is recognized as the bright yellow, orange, and purple zone of coloration directly underlying the WRG. The unconformity is capped by fluvial deposits of the Late Eocene Chamberlain Pass Formation (Evans and Terry, 1994; Terry, 1998). Although vertebrate fossils have been recovered from this unit (Vondra, 1958; LaGarry et al., 1996), they were not part of this study. The Chamberlain Pass Formation is unconformably overlain by the Late Eocene Chadron Formation.

Unlike the threefold division of the Chadron Formation in the Big Badlands of South Dakota, the Nebraska section only contains two members (Fig. 2a), the laterally extensive Peanut Peak Member and the recently defined Big Cottonwood Creek Member (Terry, 1998; Terry and LaGarry, 1998). The Peanut Peak Member is recognized as the hummocky weathered grayish green claystone and mudstone that directly overlies the Chamberlain Pass Formation. Fossils are rare within this unit. The overlying Big Cottonwood Creek Member is recognized as the more resistant and cliff-forming greenish brown unit composed of overbank mudstones, siltstones and channel sandstones (Fig. 2b). Fossils from the Chadron Formation represent the Chadronian North American Land Mammal Age (NALMA).

The Chadron Formation is overlain by the Oligocene Brule Formation. The contact is conformable and intertonguing for the most part, with the exception of the Toadstool Park channel complex which removes up to 10 m of the underlying Chadron Formation in places (Fig. 2a,b). The Eocene–Oligocene boundary (ca.

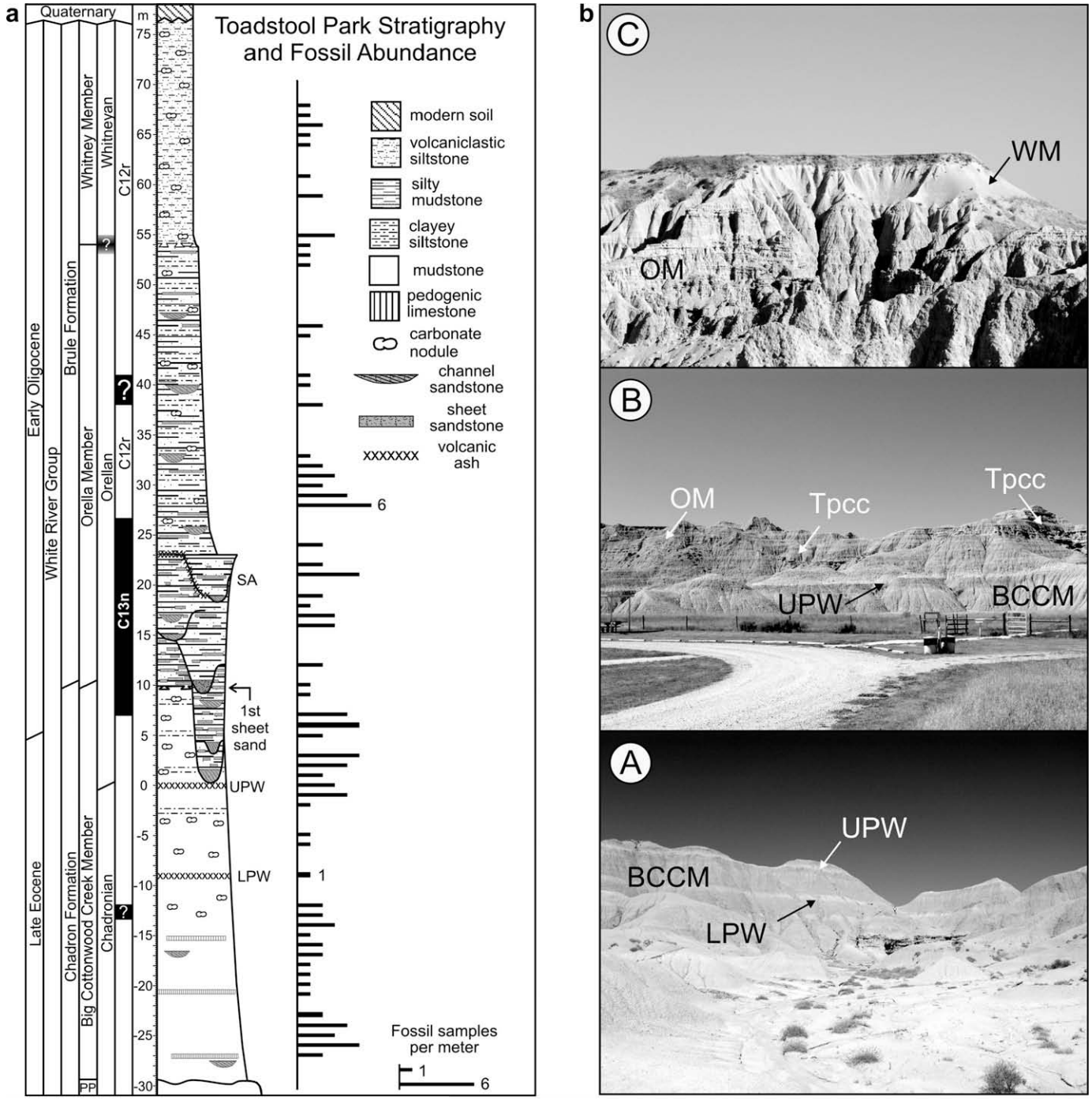

Fig. 2. (a) Measured section of the White River Group at Toadstool Geologic Park, NE. The zero elevation point is the Upper Purplish White Layer (UPW). PP = Peanut Peak Member, Chadron Formation. Other marker beds include: LPW = Lower Purplish White Layer, SA = Serendipity Ash Layer. Positions of horizontal bars indicate the stratigraphic positions of fossils sampled for this study. Length of bars indicates the number of bones obtained within a 1 m interval. (b) Outcrop photographs of stratigraphic units. (A) Big Cottonwood Creek Member (BCCM) of the Chadron Formation with the lower and upper Purplish White Layers (LPW/UPW), respectively. (B) Contact between the BCCM and early Oligocene Orella Member (OM) of the Brule Formation. The Toadstool Park channel complex (Tpcc) of the Orella Member incises into the BCCM. (C) Contact between the Orella and Whitney Members (WM) of the Brule Formation.

33.5 Ma) occurs within this uppermost 10 m of the Chadron Formation, approximately 5 m above the *Upper Purplish White Layer* (UPW) volcanic tuff (Zanazzi et al., 2007).

The Brule Formation in this region is divided into the Orella, Whitney, and informal *Brown Siltstone* Members (LaGarry, 1998). The lowermost Orella Member is characterized by interbedded beige, tan, and brown silty mudstones, siltstones and sandstones deposited in channel and overbank settings (Fig. 2b). The overlying Whitney Member is conformable and intertonguing with the Orella Member. It is a pinkish gray volcaniclastic siltstone with rare channel sandstones and numerous "*potatoball*" carbonate concretions. Both of these units are fossiliferous and represent the Orellan and Whitneyan NALMAs, respectively.

3. Previous REE research

The basis for, and use of, REE in vertebrate fossils has been extensively discussed in a number of previous publications

(Elderfield and Pagett, 1986; Wright et al., 1987; Trueman and Benton, 1997; Trueman, 1999; Trueman and Tuross, 2002; Picard et al., 2002; Trueman et al., 2003, 2005, 2006; Patrick et al., 2004; Martin et al., 2005; and references cited therein). Vertebrate bones are composed of very fine-grained, poorly crystalline, carbonate-bearing hydroxy-apatite. Bones of living organisms contain very low REE concentrations; however, after death REE are adsorbed onto apatite surfaces and incorporated into the apatite crystals as they recrystallize and grow during fossilization (Koeppenkastrop and DeCarlo, 1992; Trueman and Benton, 1997; Trueman, 1999; Trueman and Tuross, 2002; Patrick et al., 2004; Martin et al., 2005). There they are retained unless the apatite is dissolved or highly metamorphosed (Trueman, 1999; Armstrong et al., 2001). The understanding, however, of the relationship between the REE signatures of the fossil and diagenetic vadose or groundwaters and their possible paleoenvironmental implications is still limited. The REE composition and signature incorporated in a fossil depends on the fluid composition, the amount and composition of REE released or sequestered by water/rock reactions with other minerals or colloidal phases, and possibly the relative concentrations and lability of the various REE complexes. In general, basic, alkaline waters have shale-normalized signatures which are heavy REE (HREE)-enriched because of preferential complexing of HREE by dissolved carbonate (Wood, 1990; Haas et al., 1995; Johannesson and Zhou, 1997). Circum-neutral pH waters may be light-, middle-, or heavy-REE-enriched or have flat patterns with no significant fractionation (Johannesson and Zhou, 1997). Organic complexes may also affect REE patterns and concentrations in natural waters; however, their role is still poorly understood (e.g. Johannesson et al., 2004). Sedimentary materials tend to be LREE- or MREE-enriched (Nesbitt, 1979; Nesbitt and Markovics, 1997; Frey and Grandstaff, 2004). Thus, reactions with colloids, such as dissolution of hydrous ferric oxides (HFO) and pyrolucite, degradation of organic matter, and ion-exchange with clays will tend to release lanthanides enriched in LREE or MREE into solution (Erel and Stolper, 1993; Johannesson et al., 2000; Dia et al., 2000; Hannigan and Sholkovitz, 2001; Gruau et al., 2004; Patrick et al., 2004). These may then be incorporated during fossilization. Fractionation of various REE between water and fossil apatite may be small, because of their large and similar adsorption constants (e.g., Koeppenkastrop and DeCarlo, 1992; Trueman, 1999; Suarez et al., 2007b). Even if some fractionation does occur during incorporation in the apatite (Lécuyer et al., 2004), differences in REE composition between fossils must still be related to differences in the diagenetic environments. Environments differing in redox, pH, salinity, concentration of complexing ligands, or degree of weathering may produce fossils with distinctly different REE signatures or Ce anomalies (e.g., Elderfield and Pagett, 1986; Wright et al., 1987; Trueman, 1999; Metzger et al., 2004; Patrick et al., 2004; Martin et al., 2005; Anderson et al., 2007). Fossilization and REE incorporation is often accomplished within a few thousand years after death, and bones from successive stratigraphic units may contain significantly different REE patterns (Trueman, 1999; Patrick et al., 2004; Trueman and Tuross, 2002; Martin et al., 2005; Trueman et al., 2005, 2006; Suarez et al., 2007b). Therefore, the provenance of fossils which are reworked or which have poor or missing collection information may be determined by comparison of signatures with known specimens (Staron et al., 2001; MacFadden et al., 2007; Patrick et al., 2007). Erosion and mixing of fossilized materials from different localities may produce allochthonous assemblages of fossils having different REE signatures (Trueman and Benton, 1997). The degree of difference in signatures may indicate the relative extent of reworking or time averaging in various stratigraphic units (Trueman, 1999; Trueman et al., 2003; Metzger et al., 2004; Suarez et al., 2007b).

4. Methods

Fossils were collected from the Big Cottonwood Creek Member of the Chadron Formation, the Orella, and lowermost 20 m of the Whitney Member of the Brule Formation (Fig. 2). The overlying *Brown Siltstone* interval was not sampled during this project. Fossils varied from pristine, unweathered specimens to those which experienced considerable weathering and carnivore processing before burial. Most fossils analyzed had not been transported for great distances; their surfaces were not abraded and, when not processed, retained the outermost, porcelaineous layer. The most common fossils sampled included oreodonts, tortoises and rhinos. Camels, horses and brontotheres were also sampled, but less frequently. With the exception of several of the brontothere specimens, which were collected from channel or overbank splay deposits, all fossils from the Big Cottonwood Creek and Orella Members were collected from overbank facies ranging from proximal to distal settings, and weak to relatively strong pedogenic development. Fossils from the Whitney Member were all from massive, pedogenetically modified muddy siltstones, presumably of eolian or mixed eolian/overbank affinity. The distribution of fossils occurs in patches, but for the most part, the entire section is represented (Fig. 2a). How much of this distribution is a function of outcrop accessibility vs. visitor traffic and fossil theft is unknown.

Fossils were located by pedestrian survey over approximately 1 km^2, entered into a GPS database, and measured into the local stratigraphy using a Jacob's staff. Fossil sites were positioned with respect to several marker beds, including the UPW within the Big Cottonwood Creek Member of the Chadron Formation and the *Serendipity Ash* (Fig. 2a,b) within the Orella Member of the Brule Formation. Bone or bone fragments containing approximately 1 cm^3 of cortical material were collected at each site. Laterally distinct specimens from the same stratigraphic level were collected as separate specimens (Fig. 2a).

Sample preparation methods followed those of Suarez et al. (2007b). Cortical bone was separated from the specimens. Matrix was mechanically removed from the bone by probes, picks, Dremel©, and ultrasonic agitation. Bones were crushed using a mortar and pestle and cleaned of carbonate using an acetic acid solution buffered to pH 5 (Jeppsson et al., 1999). Bone powder (ca. 0.1 g) was placed in 100 mL flasks and dissolved in trace-metal-grade HNO_3 with heating, where necessary. The solution was then diluted, generally by a factor of 1000, to working levels with 2% HNO_3 with 1 ng mL^{-1} In as an internal standard. Samples were analyzed for REE, Y, U, Th, and other trace elements using a ThermoFinnigan Element 2 single collector High Resolution Sector Inductively Coupled Plasma – Mass Spectrometer (ICP-MS) at University of Maryland. Samples were introduced through a nominally 100 μL min^{-1} capillary tube and aspirated into a Cetac Aridus desolvating chamber run at 70 °C. Sensitivity was $\sim 10^6$ cps/1 ng mL^{-1} for ^{115}In. NBS phosphate rock 120 was used as a reference standard. Samples have an analytical error of $\leqslant \pm 5\%$ based on triplicate analyses. The REE were normalized to the North American Shale Composite (NASC) (Gromet et al., 1984). Following Irber (1999), the magnitude of the tetrad effects for Pr and Dy were calculated using

$$\begin{aligned} Pr_N/Pr_N^* &= Pr_N/\left(La_N^{1/3} * Nd_N^{2/3}\right) \\ Dy_N/Dy_N^* &= Dy_N/\left(Gd^{1/3} * Ho^{2/3}\right) \end{aligned} \quad (1)$$

where the subscript *N* indicates NASC-normalized values.

Possible stratigraphic periodicities in bone compositions were investigated by time-series analysis (Weedon, 2005) of REE ratios. Ages of various units within the sequence are constrained by

geomagnetic reversals (Prothero, 1996), radiometric dates on tephrostratigraphically correlated ash units (Swisher and Prothero, 1990; Obradovich et al., 1995; Larson and Evanoff, 1998), and biostratigraphic data (supplemental data from Zanazzi et al., 2007; and Matthew Kohn, pers. comm., 2008). Sedimentation rates were calculated based on linear regressions of stratigraphic elevation with age of the tephra and other marker beds. Sedimentation rates increase up section, and can be approximated by two rates, 66.2 ka/m in the Chadron Formation, and 30.7 ka/m in the Brule Formation (Fig. 2a). Relative ages of fossils were calculated based on these sedimentation rates and stratigraphic elevation of the fossils within the section. The section sampled in this study comprises about 4.15 Ma, from 35.9 to 31.7 Ma (supplemental data from Zanazzi et al., 2007). Most fossils used were found in situ and their relative ages can be calculated exactly from the sedimentation rates. Twenty-nine fossils found in float were also used in the time-series analysis. Their calculated ages are somewhat uncertain, but since the fossils were probably found within 1 m of their proper stratigraphic elevation, the errors in calculated ages (<66 ka) are much smaller than the shortest period cycle that can be observed (~200 ka) and should not affect the calculation. For time-series analysis, data must have single values for any interval. Therefore, an average value was used where multiple fossils were collected from the same bed (Fig. 2a). Periodograms were calculated using the PC program SPECTRUM (Schulz and Stattegger, 1997). SPECTRUM (Schulz and Stattegger, 1997) is based on the Lomb-Scargle Fourier transform and allows calculation of the periodogram directly from unevenly spaced data without interpolation. Siegel's (1980) test for multiple periodicities was used to determine the significance of periodogram peaks (Schulz and Stattegger, 1997). There are 101 points in the data set, including data points from bones in the same bed which were then averaged; therefore, the average interval between samples is about 40 ka.

One of the major problems with REE data is visualization of analytical results. REE concentrations or signatures of individual samples are commonly visualized as multi-element diagrams (Fig. 3) normalized to reduce the Oddo-Harkins effect; however, these cannot be used readily to delineate fractionation or evolutionary trends. Plotting ratios of two REE as a function of another variable, such as stratigraphic elevation, allows some trends to be determined (e.g., Patrick et al., 2004; Martin et al., 2005; Suarez et al., 2007b), but may miss important variations in other lanthanides. Trueman and his co-workers (e.g., Trueman, 1999; Trueman and Tuross, 2002; Trueman et al., 2006) have used bivariate plots using combinations of LREE, MREE and HREE (e.g., Sm_N/Yb_N vs. Sm_N/Pr_N and La_N/Sm_N vs. La_N/Yb_N). Patrick et al. (2004) developed a ternary plot utilizing Nd_N, Gd_N and Yb_N vertices, which allows more extensive mixing relations to be examined. However, this ternary diagram does not allow visualization of potentially important variations in La and the lightest REE. In this paper REE data are presentd in a tetrahedron (Fig. 4) having La_N–Nd_N–Gd_N–Yb_N vertices (subscript N = shale-normalized values). These four REE cover the range from light to middle and heavy rare earths. Cerium or Eu anomalies cannot be visualized with this combination of REE, but such anomalies do not appear important in TGP samples. Analytical results were normalized so that $La_N + Nd_N + Gd_N + Yb_N = 1$. Such closed data sets have limitations, but should allow qualitative evaluations of trends (Rollinson, 1993). Using the equations of Spear (1980), the tetrahedron may be rotated to any angle, allowing data trends to be visualized. The tetrahedron may also be drawn as a

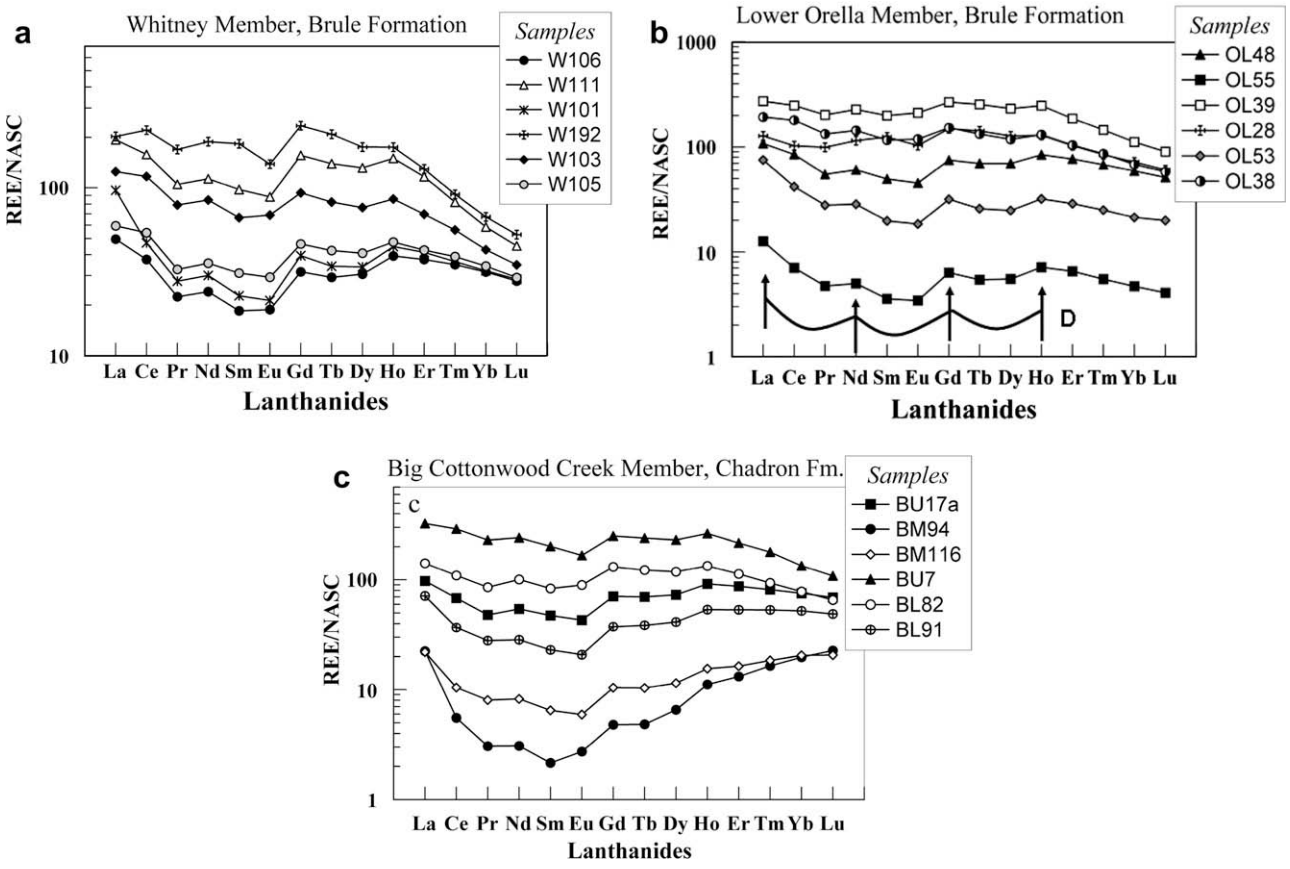

Fig. 3. Multi-element diagrams of NASC-normalized REE from individual stratigraphic units at Toadstool Geologic Park, NE. Arrows (lower Orella Member) point to intermediate knick points (Nd, Gd, and Ho) for the tetrad effect and curve D illustrates the first 3 spans of the W-type effect. NASC = North American Shale Composite (Gromet et al., 1984). NASC-normalized values were used for consistency with previous work (e.g., Metzger et al., 2004).

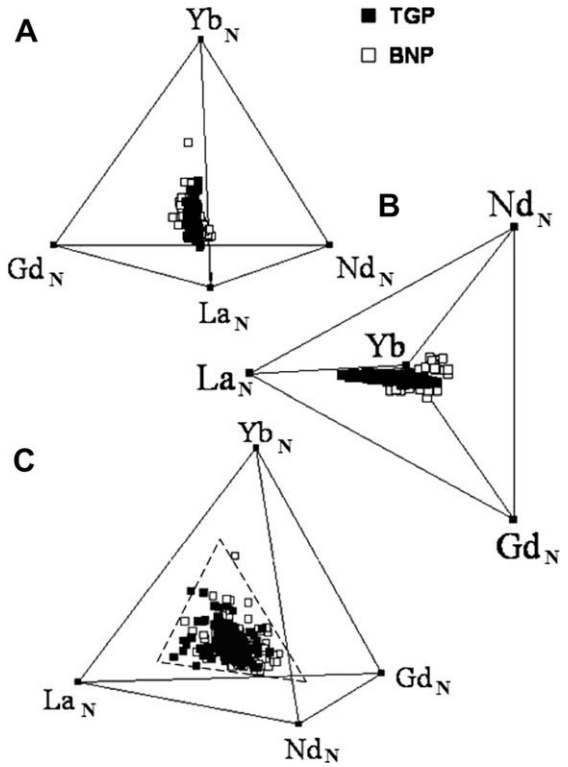

Fig. 4. Three-dimensional tetrahedral displays of NASC-normalized REE data from Toadstool Geologic Park (TGP) and Badlands National Park (BNP). Note the planar array of data within these orthogonal projections. The 3-component mixing triangle is marked in projection c.

stereo pair (Spear, 1980) or anaglyph (Purnell, 2003), for examination in 3 dimensions. Samples having flat patterns, without significant fractionation relative to NASC, will plot in the center of the tetrahedron. In contrast, samples with significant LREE enrichment will plot toward the La or Nd vertices, whereas samples enriched in HREE will plot toward the Yb vertex (see also Patrick et al., 2004).

5. Results

Results of REE analyses of fossils are available from the data repository. Representative NASC-normalized REE signatures in fossils from the Big Cottonwood Creek, Orella, and Whitney Members of the Chadron and Brule Formations are shown in Fig. 3. Normalization with NASC was chosen to facilitate comparisons with many previous studies. REE profiles differ within and between units, both in concentration (more than a factor of 10) and signature. Signatures range from LREE-enriched (e.g., BU7 and W192) to HREE-enriched (BM94) and most are MREE-depleted (e.g., W101 and 106). In most samples, Ce and Eu anomalies are small or absent. Many samples display tetrad effects (e.g. Masuda et al., 1998; Irber, 1999; Takahashi et al., 2002), which are observed as curves that break the signature into four segments consisting of La–Nd, Nd–Gd, Gd–Ho and Ho–Lu (see example in Fig. 3b). In the tetrad effect, Pr or Dy, for example, may plot above or below the lines connecting La and Nd or Gd and Ho, creating curves. Concave curvatures are called W-type tetrads and convex curves are M-type (e.g. Masuda et al., 1998; Irber, 1999; Takahashi et al., 2002); here, all curves are W-type tetrads. The origin and extent of the tetrad effect in geological samples is still a matter of discussion, but may result from inter-electron repulsion in the 4f orbitals and crystal field effects (see Kawabe et al., 1998; Irber, 1999). In TGP samples, the curvature is most clearly seen in the first and third spans (La–Nd and Gd–Ho), but the last segment (Ho–Lu) is not obviously curved.

Data from 120 TGP fossils were used in this study, including multiple bones collected from individual beds. Data are plotted (filled squares) in a La_N–Nd_N–Gd_N–Yb_N tetrahedron (Fig. 4). Data from a previous study (Metzger et al., 2004) of REE in fossils collected approximately 150 km NE of the study area from correlative sediments in Badlands National Park (BNP) (Fig. 1) are plotted (open squares) for comparison. In Fig. 4 the tetrahedron has been rotated to show three approximately orthogonal views to give the best perspective on trends and relationships in TGP data. In views A and B, data from both TGP and BNP plot along or near a common line that approximately bisects the Gd_N–Nd_N axis. The linear arrays indicate that mixing or evolutionary trends are similar for the two areas. Data from both TGP and BNP fossils have very similar and approximately constant Gd_N/Nd_N ratios. View C shows that the data are arranged in a triangle, approximately in the La_N–Yb_N–(Gd_N–Nd_N) plane. This is emphasized in Fig. 5, in which La_N, Nd_N and Yb_N data from TGP and BNP plot near a common plane in a triangular array, indicating 3-component mixing or evolution between HREE, MREE and LREE-enriched end-members. Closeness to the common regression plane is shown by short drop lines from the data to the regression plane. Because the TGP and BNP fossils have very similar and approximately constant Gd_N/Nd_N ratios, a plot of La_N–Gd_N–Yb_N would be virtually identical. Similar results can be obtained by plotting the data in multiple triangular diagrams (e.g., Nd_N–Gd_N–Yb_N and La_N–Gd_N–Yb_N). However, because the data are not exactly perpendicular to or parallel with those planes, points projected onto those planes would be somewhat more scattered, broadening the trends and obscuring slightly the relationships of the data.

TGP data cluster tightly about the line, whereas BNP data have slightly greater scatter (Fig. 4). All of the TGP samples were collected from an area of approximately 1 km^2, whereas BNP samples were collected over a distance of 50 km but within a more restricted stratigraphic range (Scenic Member of the Brule Formation, Metzger et al., 2004). Further, BNP fossils were obtained from both pedogenic and non-pedogenic sediments (Metzger et al., 2004).

The magnitudes of the tetrad effects (Equation (1)) for Pr (Pr_N/Pr^*_N) and Dy (Dy_N/Dy^*_N) in TGP samples are plotted in Fig. 6. Given an analytical uncertainty of ca.±5%, tetrad values <0.9 (W-type) are analytically significant (Irber, 1999; Monecke et al.,

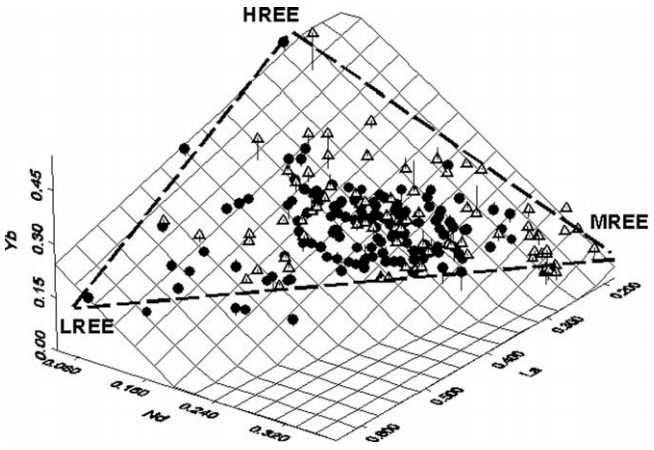

Fig. 5. La_N–Nd_N–Gd_N plot of REE data with regression plane showing the triangular, planar array of data. Data from Toadstool Geologic (●) and Badlands National (Δ) Parks. Data from TGP and BNP plot close to a common regression plane, note short drop lines. Because the Gd_N/Nd_N ratio is approximately constant in both data sets, a plot of La_N–Gd_N–Yb_N would appear very similar. The general, 3-component mixing triangle for TGP and BNP samples is shown on the plane. HREE = Heavy rare earth enriched, MREE = Middle rare earth enriched, LREE = Light rare earth enriched.

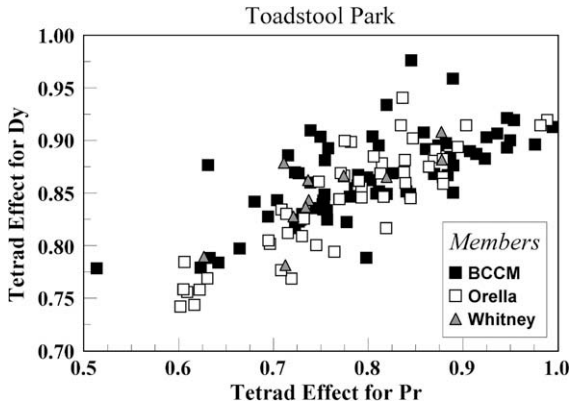

Fig. 6. Tetrad effects for Pr (Pr_N/Pr_N^*) and Dy (Dy_N/Dy_N^*) (Equation (1)) for 3 members of the Chadron and Brule Formation at TGP. BCCM = Big Cottonwood Creek Member, Chadron Formation.

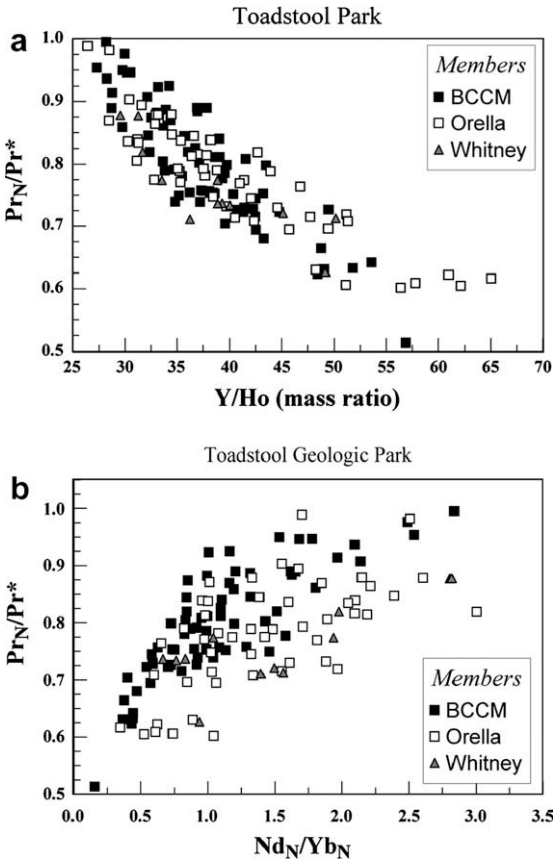

Fig. 7. Tetrad effect for Pr (Pr_N/Pr_N^*) vs. Y/Ho mass ratio (a) and Nd_N/Yb_N (b) for TGP. BCCM = Big Cottonwood Creek Member, Chadron Formation.

2003). Therefore, many samples have significant W-type tetrad effects for the first and third tetrads with the tetrad effect for Pr being slightly greater. Groundwaters generally have greater W-type tetrad values than do co-existing sediments and the sediments or residual phases may develop complementary M-type tetrad values (Takahashi et al., 2002; Gimeno et al., 2007), which are not observed here. Although W-type tetrads may form in acidic river waters (Gimeno et al., 2007), the effect appears more common in alkaline waters and seawater (Masuda et al., 1998; Takahashi et al., 2002). The W-type tetrad effect in solution appears to result from carbonate complexing in basic solutions; equilibrium with colloids, such as ferric oxyhydroxides; slightly reducing conditions, and relatively restricted water/rock ratios (Masuda et al., 1998; Kawabe et al., 1998, 1999; Bau, 1999; Takahashi et al., 2002; Gimeno et al., 2007).

Tetrad values for Pr correlate significantly with the Y/Ho mass ratios and Nd_N/Yb_N (Fig. 7). A correlation between tetrad values and Y/Ho mass ratio has previously been found by Irber (1999), in evolved granites, and Takahashi et al. (2002), in sediments and groundwaters. The Y/Ho mass ratio in chondrites, average shale, and average upper crust is approximately 28 (Taylor and McLennen, 1985; Irber, 1999); however, the Y/Ho ratio in TGP samples ranges from about 28 to 65 (Fig. 7a). Yttrium and Ho have the same ionic charge and essentially the same ionic radii (Shannon and Prewitt, 1969; Irber, 1999) and should not fractionate from one another except as a result of differences in aqueous complexing (Bau and Dulski, 1995). The association constant for the $YF_{(aq)}$ complex is larger than that for Ho and most other REE (Walker and Choppin, 1967); therefore, Bau and Dulski (1995) suggested that preferential formation of YF complexes could account for increased Y/Ho ratios in solution. However, in experiments, scavenging of REE and Y by precipitating HFO also produced positive fractionation of La and Y relative to other REE (Bau, 1999), and it is possible that complexes with other ligands, including organic ligands, might produce such fractionations. Therefore, the origin of the Y/Ho fractionation in these samples is conjectural.

Tetrad values for Pr (and Dy) also correlate with Nd_N/Yb_N (Fig. 7b) and Gd_N/Yb_N ratios. Fossils with large tetrad values ($Pr/Pr^* \ll 1$) are HREE-enriched ($Nd_N/Yb_N < 1$) whereas fossils with smaller tetrad values ($Pr/Pr^* \sim 1$) are MREE- and LREE-enriched (e.g., $Nd_N/Yb_N > 1$).

In most previous studies, interpretations were drawn only from the shape of the REE profile or from ratios of REE, not from REE concentrations (e.g., Trueman and Benton, 1997; Trueman, 1999; Trueman and Tuross, 2002; Trueman et al., 2005; Patrick et al., 2004; Suarez et al., 2007b). REE concentrations may vary with depth in bone with high concentrations near the surfaces and lower concentrations in the interior of the cortical layer (Henderson et al., 1983; Trueman and Tuross, 2002; Trueman et al., 2006). The cortical samples analyzed in this study should integrate most of the REE added to the bone during fossilization (Trueman et al., 2006). Concentrations of total REE (∑REE) (dominated by concentrations of Ce and La) in TGP samples correlate significantly with differences in REE ratios (e.g., Y/Ho mass ratio and Nd_N/Yb_N, and the tetrad effect) (Fig. 8).

Although there is considerable variability in the data, essentially all of the REE_N/Yb_N ratios, such as the Nd_N/Yb_N ratio (Fig. 9), Gd_N/Yb_N, and La_N/Yb_N, and their variances increase upward in the section. For example, for Nd_N/Yb_N, both the *t*-test and Mann–Whitney tests indicate that the Nd_N/Yb_N ratio is significantly greater in the upper part of the section (above the Upper Purplish White (UPW) marker bed, Fig. 2a) (Aspin-Welch Unequal-Variance test, $t = 8.16$, $p < 0.001$, $N_{lower} = 28$, $N_{upper} = 92$) and the F and Modified Levene Equal Variance tests confirm that the variance of data from the upper part of the section is significantly greater than for the lower part ($F = 5.34$, $p < 0.001$). These statistical tests indicate that the signatures become progressively LREE- and MREE-enriched and more variable toward the top of the section.

6. Interpretation

Trueman and Tuross (2002) and Trueman et al. (2006) have found that, in some samples, REE concentrations decrease with depth in cortical layers of the bone and that, at least in those samples, REE are fractionated, with more HREE-enriched patterns at

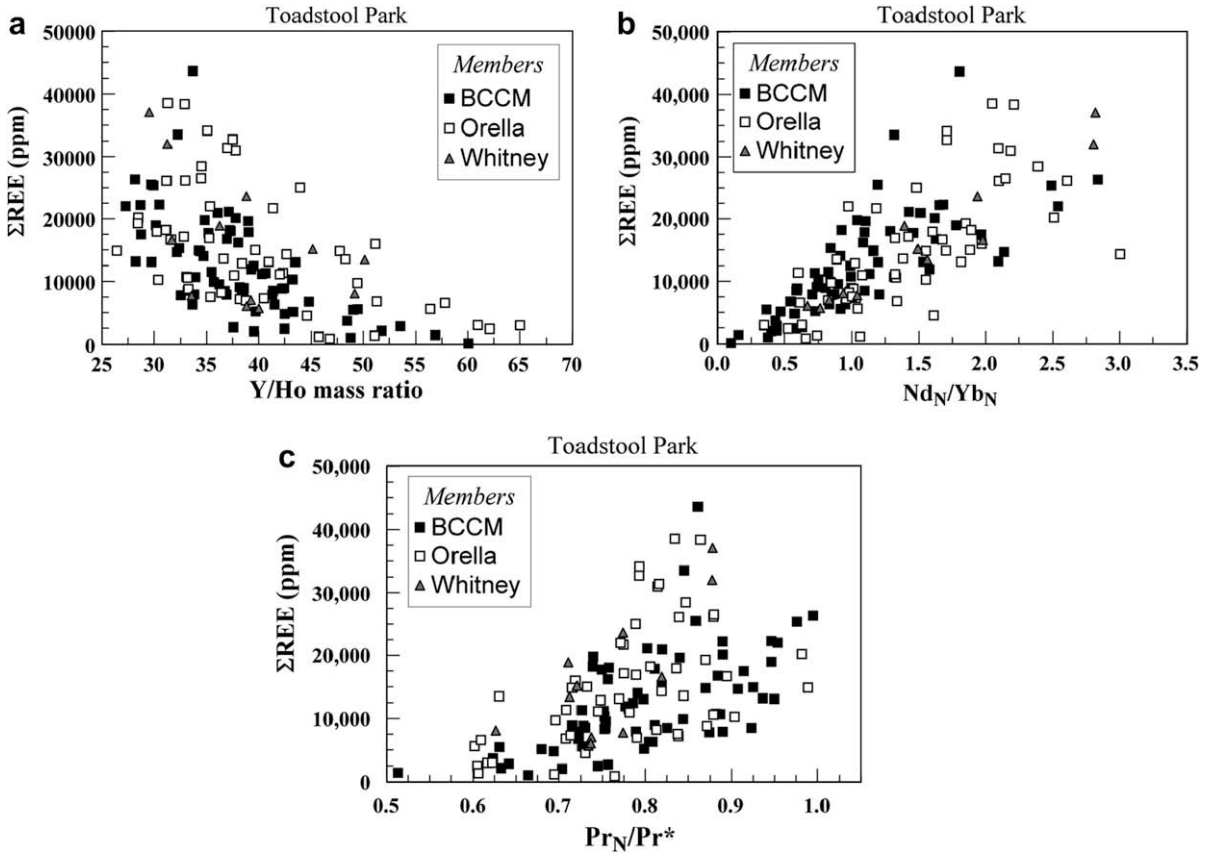

Fig. 8. Total REE ($\sum$REE) and Y/Ho (a), Nd_N/Yb_N (b), and tetrad effect for Pr (Pr_N/Pr^*_N) (c), for TGP specimens from the 3 members. BCCM = Big Cottonwood Creek Member, Chadron Formation.

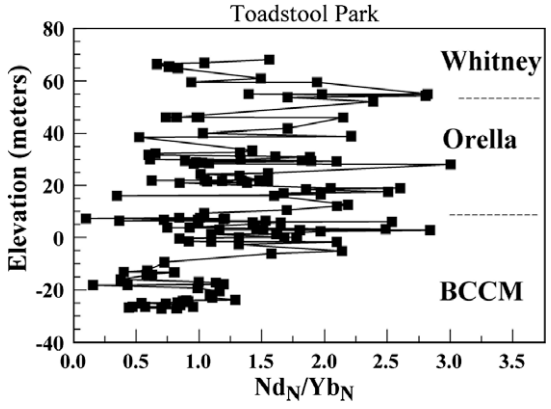

Fig. 9. NASC-normalized Nd_N/Yb_N as a function of stratigraphic position at TGP. The zero elevation point is the Upper Purplish White Layer. The Nd_N/Yb_N ratio increases with elevation and the amount of variation in the ratio increases above approximately zero elevation. BCCM = Big Cottonwood Creek Member, Chadron Formation.

depth (see Trueman and Tuross, 2002, Fig. 5). It has been suggested that inclusion of variable amounts of deeper, HREE-enriched cortical material could account for the patterns seen in the present specimens. However, preliminary analyses of transects across TGP bones (unpublished data) suggest that REE concentration gradients near the bone surface or around Haversian canals are small or absent in the TGP samples. Similarly, Suarez et al. (2007a) have also found small concentration gradients with small degrees of REE fractionation in *Falcarius utahensis* bones from the early Cretaceous Crystal Geyser Dinosaur Quarry. Therefore, near-surface concentration gradient REE fractionation may not be present in all fossil bones. Further, even if large concentration gradients and REE fractionations were present in TGP samples, the resulting trends would be different from those observed. Although bulk REE concentrations obtained by solution ICP-MS will be diluted by inclusion of greater amounts of deep cortical material, REE and TE ratios will be dominated by ratios in the higher concentration, surface layers. Inclusion of greater amounts of deep cortical material will result in curvilinear REE concentration/ratio trends, similar to hyperbolic dilution curves, much different than trends seen in Fig. 8. Finally, based on data from (Trueman and Tuross, 2002, Fig. 5), the trend generated should approximate a 2-component mixing line running from a Yb_N-enriched member nearly perpendicular to the La_N–Nd_N–Gd_N plane, rather than the 3-component mixing observed in TGP samples. Therefore, the data do not appear compatible with a concentration-gradient, depth-dependent sampling model; most of the variation in REE seen in this study must be related to temporal and spatial variations in fluid chemistry.

REE in fossils from TGP and BNP plot in a triangular region of the La_N–Nd_N–Gd_N–Yb_N tetrahedron (Figs. 4 and 5), indicating that REE compositions from both areas result from 3-component mixing or evolution. Samples plotting toward Yb are HREE-enriched. Alkaline, high pH waters tend to be HREE-enriched (e.g. Johannesson and Zhou, 1997) because carbonate complexation favors HREE solubility. Thus, bones incorporating REE exclusively from alkaline waters will have HREE-enriched patterns. In contrast, most sedimentary materials, including hydrous ferric oxides (HFO) and Mn oxides, clays and organic matter, are relatively LREE- and MREE-enriched. If these LREE and MREE are released from the HFOs and other minerals into vadose or groundwaters during weathering, ion exchange, or reductive dissolution and then incorporated

from solution into the fossilizing bones, the bones will have LREE- or MREE-enriched patterns. The REE relationships observed in the TGP and BNP fossils are best explained by a 3-component interaction between HREE-enriched (low Nd_N/Yb_N ratio), alkaline, high pH vadose or groundwater with large W-tetrad effect ($Pr_N/Pr_N^* < 1$, equation (1) and Irber, 1999) and high, non-chondritic Y/Ho mass ratio, and REE released from two sedimentary components enriched in LREE and MREE (higher Nd_N/Yb_N and Gd_N/Yb_N ratios) with lower, near-chondritic Y/Ho ratios and small tetrad effects ($Pr_N/Pr_N^* \sim 1$). Thus, in Fig. 7a and b, for example, TGP fossils with HREE-enriched (low Nd_N/Yb_N and Gd_N/Yb_N ratios) signatures, high W-tetrad values ($Pr_N/Pr_N^* < 1$), and non-chondritic Y/Ho ratios probably obtained most of their REE from alkaline waters, whereas fossils with MREE- or LREE-enriched signatures, small or non-significant tetrad values ($Pr_N/Pr_N^* \sim 1$), and near-chondritic Y/Ho ratios must have obtained most of their REE from reactive sedimentary components, such as volcanic ash or hydrous ferric oxides.

These patterns may also be consistent with $\sum$REE correlations (Fig. 8). Most groundwaters have very low REE concentrations, in the low pmol/kg range (e.g., Johannesson and Zhou, 1997); bones taking up REE mostly from groundwater during fossilization might be expected to have low REE concentrations and signatures characteristic of the groundwater, whereas fossils obtaining REE from both groundwater and additional reactive colloid sources might have higher REE concentrations (assuming similar periods of fossilization and fluid fluxes) and signatures more similar to those of the reactive sedimentary components. Differing proportions of REE input from water and reactive sedimentary components will produce mixing or evolutionary lines or planes between end-members. Sedimentary components responsible for LREE- and MREE-enrichment have not yet been identified. Some, though not all, of the La-enriched samples are near ash beds.

Although the tetrad effect is found in many TGP fossils, the effect is smaller or non-significant in most BNP fossils (Metzger et al., 2004). Thus, although the mixing end-members are similar for both TGP and BNP, there may have been differences in the composition of sediments and groundwaters during fossilization at the two localities.

The Nd_N/Yb_N ratio and other REE_N/Yb_N ratios and their variances are significantly greater in the OM than in the BCCM (Fig. 9). Overall, REE signatures become more LREE- and MREE-enriched and more variable up section in the Brule Formation. Zanazzi et al. (2007) found that, based on $\delta^{18}O$ values in bone carbonate, mean annual temperatures decreased by a maximum of 8 °C from the Eocene to Oligocene. Therefore the shift in REE signatures and REE ratios in TGP fossils may indicate that they may represent a climate proxy.

The precise mechanisms for such a shift in REE signatures must still be determined, but might result from decreased precipitation and flux of groundwater higher in the section and, therefore, increased relative importance of REE additions from sedimentary components. It is also possible that changes in protolith and paleosol characteristics, such as increased abundance of glass from volcanic ash or a period of paleosol formation, could also alter the water/rock ratios, producing more LREE-enriched patterns in fossils.

Assuming that the incorporation of REE is primarily a near surface, meteoric event, it is plausible that changes in pedogenic processes may be partly responsible for the up-section shift in REE signatures, similar to those described by Metzger et al. (2004). Paleosols change up section from forested alfisols within the Peanut Peak Member at the base of the Chadron Formation to mollisol-like soils near the top of the BCCM (Retallack, 1983; Terry, 2001). These changes are associated with lesser degrees of alteration of volcaniclastic grains, translocated clays, a reduction in the amount of carbonate accumulation, and a change to progressively smaller mean root sizes (Terry, 2001). Paleosols of the Orella Member are weakly developed fluvents and inceptisols. Paleosols of the Whitney Member are cumulic in nature and contain vertically oriented root traces, presumably in response to drier climatic conditions and the need for deeply penetrating roots. Meehan (1994) analyzed paleosols within the Whitney Member and concluded that, based on petrographic and geochemical analyses, the Whitney Member represented eolian deposition with episodes of weak pedogenic development. Meehan (1994) noted earthworm burrows, sweat bee larvae, fecal pellets, silicified plant fragments and phytoliths.

When fossils were collected, they were identified, where possible, and their taphonomic characteristics and degree and type of processing were determined (Fig. 10a). Types of fossil processing (post-mortem modifications to the bone surface) identified include: weathering, gnaw marks from rodents, and root etching. Fig. 10b shows, as an example, the Nd_N/Yb_N ratio of fossils as a function of elevation, fossil type (mammal and tortoise) and degree of processing. Although there is considerable variability in the data, there are no significant differences in the Nd_N/Yb_N or other ratios related to fossil type (several tortoise and mammal species), degree of weathering or processing. Fossil type and taphonomic history appear to have had little to no effect on REE signatures, and thus can be ruled out as a possible influence on geochemical variability (Fig. 10b).

If the REE composition of fossils is influenced by climate, as suggested by the overall trend in Nd_N/Yb_N, for example, the high degree of variability in Nd_N/Yb_N (Fig. 9), Gd_N/Yb_N, La_N/Yb_N and other REE ratios with stratigraphic elevation, particularly above ca. 0 m (Figs 2b, 9), may reflect periodic shorter-term climate fluctuations and paleoenvironmental changes. Fig. 11 shows a periodogram generated by spectral analysis of the Nd_N/Yb_N ratio using SPECTRUM (Schulz and Stattegger, 1997). Siegel's (1980) test indicates significant periodicities at ca. 1050, 800, 570, 440 and 225 ka. Cycles calculated from the Gd_N/Yb_N and La_N/Yb_N ratios are similar. These periods are similar to modulations of Milankovitch-band astronomical, climate fluctuation, and stratigraphic periodicities found in previous studies (e.g., Fischer, 1982). For example, Berger (1977) found modern astronomical cycles of ca. 1310, 600, 413 and 260 ka and Tiwari (1987) found isotopic cycles of ca. 1250, 800 and 400 ka.

Although similar, the periodicities calculated do not correspond exactly with the longer-term astronomical Milankovitch cycles or their modulations (e.g., Berger, 1977). It is possible that Oligocene climate cycles in the North American interior were modified by local or regional orographic effects (Zanazzi et al., 2007); however, the discrepancy might also be due to errors in sedimentation rate, hiatuses, or aliasing due to inadequate sampling frequency (e.g., Weedon, 2005). More extensive sampling, perhaps over longer stratigraphic ranges, as well as reconsideration of the depositional rates may be necessary.

Because time-series analysis requires that each interval have only a single value, an average REE ratio was used where multiple fossils were collected from the same bed (Fig. 2a). In many cases, REE ratio values for the fossils were similar to one another and to the average (Fig. 10). However, Trueman et al. (2006) have shown that REE signatures in fossils can vary significantly along a land surface, even within a few meters lateral distance. In such cases, an average REE value may not be representative and time series analysis of such data may not be valid. If the bones in this study were randomly chosen, non-representative samples from a varying paleosurface, it seems unlikely that significant periodicities would be obtained. However, additional lateral sampling of fossils should be done at TGP to determine the amount of variability within individual horizons.

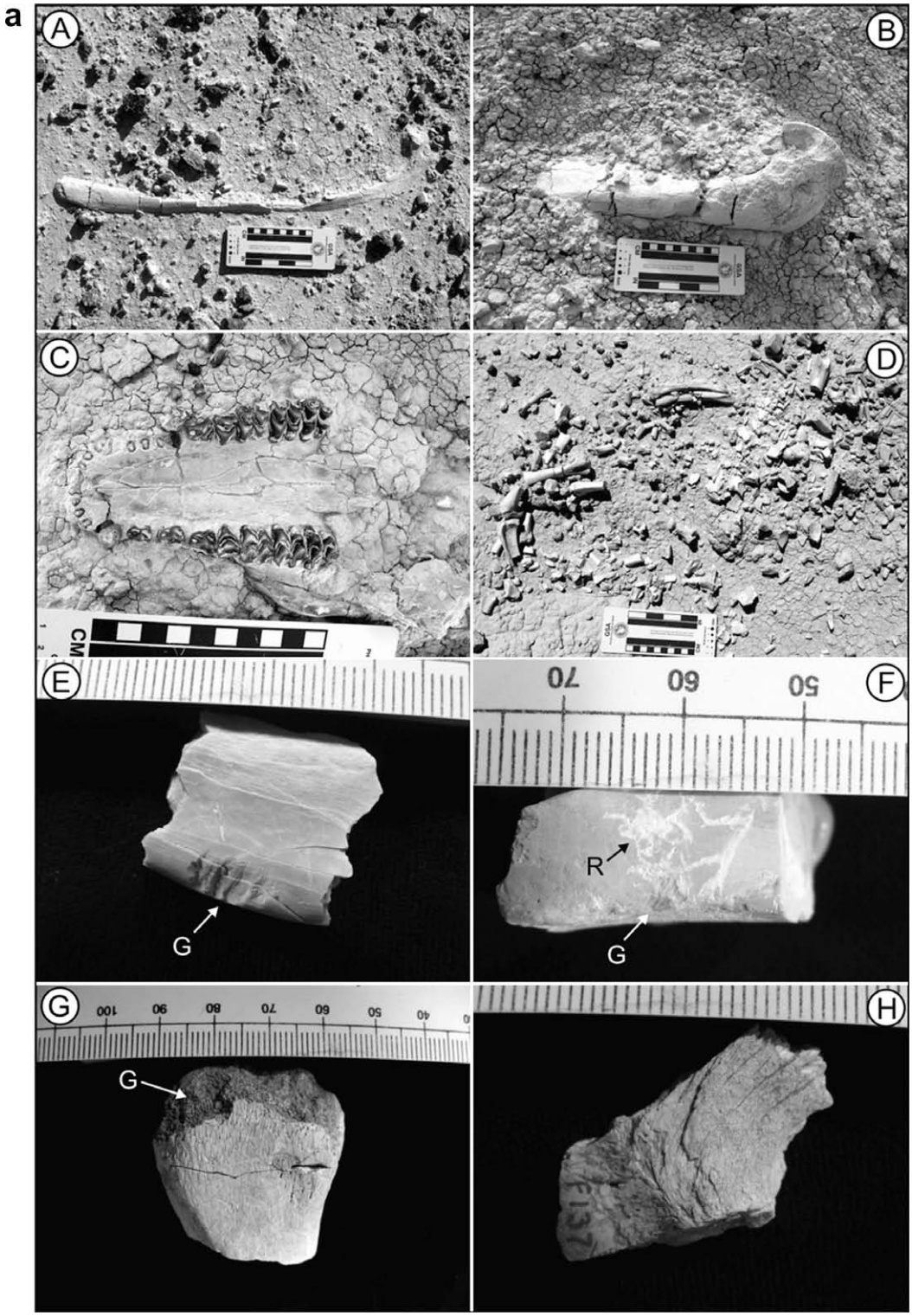

Fig. 10. (a) Photographs of vertebrate fossils from TGP and associated taphonomic features. (A): Isolated brontothere rib bone from the Big Cottonwood Creek Member (BCCM, ca.−27 m level of Fig. 2a). (B): Isolated brontothere limb bone from the BCCM (ca. -14 m of Fig. 2a). (C): Associated inverted oreodont skull from the upper part of the BCCM. (D): Articulated skeleton within the Orella Member (OM). (E): Rodent gnaw marks (G) on a jaw fragment from the BCCM (ca. 4 m level of Fig. 2a, otherwise fresh bone). (F): Rodent gnaw marks (G) and root etching (R) on a limb bone fragment from the BCCM (0 m level of Fig. 3a). (G): Heavily gnawed (G) articular surface of a tortoise limb bone from the OM (ca. 1.5 m below the Serendipity Ash of Fig. 2a). (H): Fragment of tortoise carapace, heavily weathered before fossilization, collected from an outwash channel at the base of the badlands exposures. (A-D) – Scale bars in centimeters and inches. (E) and (F) – Scale in mm. (b) NASC-normalized Nd_N/Yb_N ratios as a function of stratigraphic position, fossil type, and degree of taphonomic processing. Bones with large symbols have been processed, having their surfaces altered by weathering or gnawing prior to fossilization. Small symbols indicate bones that have not been processed.

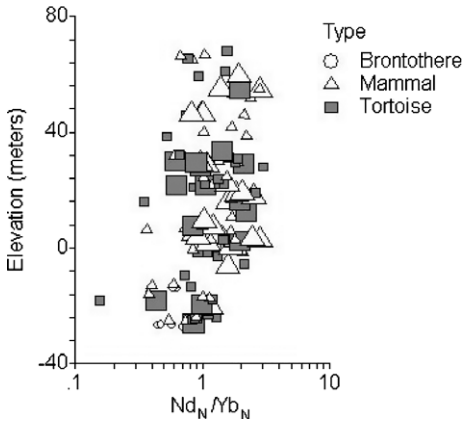

Fig. 10 (*continued*)

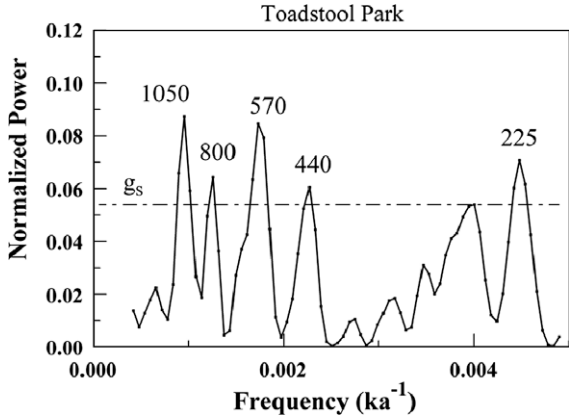

Fig. 11. Spectral frequency plot of Nd_N/Yb_N data for fossils from TGP. Line g_s marks the critical value ($g_s = 0.052$, $\alpha = 0.05$) for Siegel's (1980) test for multiple periodicities (Schulz and Stattegger, 1997). Peaks greater than the critical value are statistically significant and their periods are labeled.

7. Conclusions

The REE composition of fossils from TGP and BNP result from 3-component reactions between HREE-enriched alkaline vadose or groundwater, conducive to fossil preservation, and two LREE and MREE enriched sedimentary components. LREE- and MREE-enriched sedimentary sources and possible paleoenvironmental implications must still be determined. Other fossil localities may exhibit different mixing patterns; for example, the REE patterns of fossils in the marine Cretaceous Pierre Shale (Patrick et al., 2004) and terrestrial Cretaceous Judith River Group and Two-Medicine Formations (Trueman, 1999) also appear to be produced largely by 3-component mixing. However, REE signatures in fossils from the Cretaceous of Tunisia (Anderson et al., 2007), Pleistocene and Holocene lacustrine deposits of Fossil Lake, Oregon (Martin et al., 2005), and the marine KT boundary of New Jersey (Staron et al., 2001) do not have separate La variations and appear to result primarily from 2-component mixing. Finally, REE in fossils from the early Cretaceous of Utah (Suarez et al., 2007b) display complex mixing in which two adjacent beds display 3-component mixing with different end-members.

Variations in REE ratios and variances in WRG fossils at TGP may be related to climate change from "greenhouse" to "icehouse" conditions across the Eocene–Oligocene boundary and progressively greater degrees of climatic or environmental variability. Signatures and trends in REE ratios are independent of animal type or taphonomic history. Nd_N/Yb_N and other REE ratios have significant periodicities of ca. 1050, 800, 570, 440 and 225 ka, similar to some Milankovitch-band orbital forcing frequencies. Because vertebrate fossils are rarer, more difficult to collect, and more unevenly distributed, it is unlikely that they can be used to delineate shorter-term Milankovitch cycles; however, they may be useful to investigate longer periodicities. These results suggest that REE within vertebrate fossils may represent a new proxy for paleoclimatic and paleoenvironmental analysis, but additional data, both lateral and vertical to the current study interval, are required to test this hypothesis.

Acknowledgments

We thank Matthew Kohn, Allesandro Zanazzi, David Fox, Jason Mintz and Gary Stinchcomb for help with field work. We thank Barbara Beasley (US Forest Service) for funding and logistical support. Richard Ash aided ICP-MS analyses. The manuscript was greatly improved by comments from Nancy Hinman, Clive Trueman and an anonymous reviewer. Time series analysis was aided by discussions with William Wei. This research was supported by Nebraska National Forest Participating Agreement 05-PA-11020700 to Temple University.

Appendix A. Supplementary material

Supplementary data associated with this article can be found, in the online version, at doi:10.1016/j.apgeochem.2008.12.027.

References

Anderson, P.E., Benton, M.J., Trueman, C.N., Paterson, B.A., Cuny, G., 2007. Palaeoenvironments of vertebrates on the southern shore of Tethys; the nonmarine early cretaceous of Tunisia. Palaeogeog. Palaeoclimatol. Palaeoecol. 243, 118–131.

Armstrong, H.A., Pearson, D.G., Griselin, M., 2001. Thermal effects on rare earth element and strontium isotope chemistry in single conodont elements. Geochim. Cosmochim. Acta 54, 435–441.

Bau, M., 1999. Scavenging of dissolved yttrium and rare earths by precipitating iron oxyhydroxide: experimental evidence for Ce oxidation, Y–Ho fractionation, and lanthanide tetrad effect. Geochim. Cosmochim. Acta 63, 67–77.

Bau, M., Dulski, P., 1995. Comparative study of yttrium and rare-earth element behaviours in fluorine-rich hydrothermal fluids. Contrib. Mineral Petr. 119, 219–230.

Berger, A.L., 1977. Support for the astronomical climatic change. Nature 269, 44–45.

Clark, J., 1975. Controls of sedimentation and provenance of sediments in the Oligocene of the central Rocky Mountains. In: Curtis, B. (Ed.), Cenozoic History of the Southern Rocky Mountains, vol. 144. Geol. Soc. Am. Mem., pp. 95–117.

Dia, A., Gruau, G., Olivie-Lauquet, G., Riou, C., Molenat, J., Curmi, P., 2000. The distribution of rare earth elements in groundwaters; assessing the role of source-rock composition, redox changes and colloidal particles. Geochim. Cosmochim. Acta 64, 4131–4151.

Elderfield, H., Pagett, R., 1986. REE in ichthyoliths: variations with redox conditions and depositional environment. Sci. Total Environ. 48, 175–197.

Erel, Y., Stolper, E.M., 1993. Modeling of rare-earth element partitioning between particles and solution in aquatic environments. Geochim. Cosmochim. Acta 57, 513–518.

Evanoff, E., 1990. Late Eocene and early oligocene paleoclimates as indicated by the sedimentology and nonmarine gastropods of the White River formation near Douglas, Wyoming. Ph.D. Thesis, Boulder, Univ. Colorado.

Evanoff, E., Prothero, D.R., Lander, R.H., 1992. Eocene–Oligocene climatic change in North America: the White River formation near Douglas, east-central Wyoming. In: Prothero, D.R., Berggren, W.A. (Eds.), Eocene–Oligocene Climatic and Biotic Evolution. Princeton University Press, Princeton, NJ, pp. 116–130.

Evans, J.E., Terry Jr., D.O., 1994. The significance of incision and fluvial sedimentation in the basal White River Group (Eocene–Oligocene), Badlands of South Dakota, USA. Sed. Geol. 90, 137–152.

Evans, J.E., Welzenbach, L.C., 1998. Episodes of carbonate deposition in a siliciclastic-dominated fluvial sequence, Eocene-Oligocene White River Group, South Dakota and Nebraska, In: Terry Jr., D.O., LaGarry, H.E., Hunt Jr., R.M. (Eds.), Depositional Environments, Lithostratigraphy, and Biostratigraphy of the White River and Arikaree Groups (late Eocene to early Miocene, North America), Geol. Soc. Am. Spec. Paper 325, pp. 93–116.

Factor, L.A., Terry Jr., D.O., 2002. A paleosol and taphonomy comparison between the Brian Maebius site and other fossil-rich localities in Badlands National Park South Dakota. Geol. Soc. Am. Abstr. with Prog. 34, A-71.

Fischer, A.G., 1982. Long-term climatic oscillations recorded in stratigraphy. In: Climate in Earth History. National Academy Press, Washington, D.C., pp. 97–104.

Frey, J., Grandstaff, D.E., 2004. The distribution of rare earth and trace elements in fractions of marine shale. Geol. Soc. Am. Abstr. with Prog. 36, 41.

Gimeno, M.J., Auqué, L.F., Gomez, J.B., 2007. Evidence of W- and M-type tetrad effects in acidic water systems. In: Bullen, T.D., Wang, Y. (Eds.), Water–Rock Interaction, vol. 12. Taylor & Francis, London, pp. 1231–1234.

Gromet, L.P., Dymek, R.F., Haskin, L.A., Korotev, R.L., 1984. The North American shale composite: its composition, major, and trace element characteristics. Geochim. Cosmochim. Acta 48, 2469–2482.

Gruau, G., Dia, A., Olivié-Lauquet, G., Davranche, M., Pinay, G., 2004. Controls on the distribution of rare earth elements in shallow groundwaters. Water Res. 38, 3576–3586.

Haas, J.R., Shock, E.L., Sassani, D.C., 1995. Rare earth elements in hydrothermal systems; estimates of standard partial molal thermodynamic properties of aqueous complexes of the rare earth elements at high pressures and temperatures. Geochim. Cosmochim. Acta 59, 4329–4350.

Hannigan, R.E., Sholkovitz, E.R., 2001. The development of middle rare earth element enrichments in freshwaters: weathering of phosphate minerals. Chem. Geol. 175, 495–508.

Henderson, P., Marlow, C.A., Molleson, T.I., Williams, C.T., 1983. Patterns of chemical change during bone fossilization. Nature 306, 358–360.

Hutchinson, J.H., 1992. Western North American reptile and amphibian record across the Eocene/Oligocene boundary and its climatic implications. In: Prothero, D.R., Berggren, W.A. (Eds.), Eocene–Oligocene Climatic and Biotic Evolution. Princeton University Press, Princeton, NJ, pp. 451–463.

Irber, W., 1999. The lanthanide tetrad effect and its correlation with K/Rb, Eu/Eu*, Y/Ho, and Zr/Hf of evolving per-aluminous granite suites. Geochim. Cosmochim. Acta 63, 489–508.

Ivany, L.C., Nesbitt, E.A., Prothero, D.R., 2003. The marine Eocene–Oligocene transition: a synthesis. In: Prothero, D.R., Ivany, L.C., Nesbitt, E.A. (Eds.), From Greenhouse to Icehouse the marine Eocene–Oligocene Transition. Columbia University Press, New York, pp. 522–534.

Jeppsson, L., Anchus, R., Fredholm, D., 1999. The optimal acetate buffered acetic acid technique for extracting phosphatic fossils. J. Paleontol. 73, 964–972.

Johannesson, K.H., Zhou, X., 1997. Geochemistry of the rare earth elements in natural terrestrial waters; a review of what is currently known. Chinese J. Geochem. 16, 20–42.

Johannesson, K.H., Tang, J., Daniels, J.M., Bounds, W.J., Burdige, D.J., 2004. Rare earth element concentrations and speciation in organic-rich blackwaters of the Great Dismal Swamp, Virginia, USA. Chem. Geol. 209, 271–294.

Johannesson, K.H., Zhou, X., Guo, Caixia, Stetzenbach, K.J., Hodge, V.F., 2000. Origin of rare earth element signatures in groundwaters of circumneutral pH from Southern Nevada and Eastern California, USA. Chem. Geol. 164, 239–257.

Kawabe, I., Toriumi, T., Ohta, A., Miura, N., 1998. Monoisotopic REE abundances in seawater and the origin of seawater tetrad effect. Geochem. J. 32, 213–229.

Koeppenkastrop, D., DeCarlo, E.H., 1992. Sorption of rare earth elements from seawater onto synthetic mineral particles: an experiment approach. Chem. Geol. 95, 251–263.

LaGarry, H.E., 1998. Lithostratigraphic revision and redescription of the brule formation, White River Group, Western Nebraska. In: Terry, D.O., Jr., LaGarry, H.E., Hunt, R.M. (Eds.), Depositional Environments, Lithostratigraphy, and Biostratigraphy of the White River and Arikaree Groups (Late Eocene to Early Miocene, North America), vol. 325. Geol. Soc. Am. Spec. Paper, pp. 63–91.

LaGarry, H.E., LaGarry, L.A., Terry Jr., D.O., 1996. New vertebrate fauna from the base of the Chamberlain Pass Fm. (Eocene), Sioux County, Nebraska. In: Proceedings of the 106th Ann. Nebraska Acad. Sci., Earth Sci. Section.

Larson, E., Evanoff, E.E., 1998. An overview of the tuffs of the White River sequence. In: Terry, D.O., Jr., LaGarry, H.E., Hunt, R.M. (Eds.), Depositional Environments, Lithostratigraphy, and Biostratigraphy of the White River and Arikaree Groups (Late Eocene to Early Miocene, North America), vol. 325. Geol. Soc. Am. Spec. Paper, pp. 1–14.

Lécuyer, C., Reynard, B., Grandjean, P., 2004. Rare earth element evolution of Phanerozoic seawater recorded in biogenic apatites. Chem. Geol. 204, 63–102.

MacFadden, B.J., Labs-Hochstein, J., Hulbert Jr., R.C., Baskin, J.A., 2007. Revised age of the late Neogene terror bird (Titanis) in North America during the Great American interchange. Geology 35, 123–126.

Martin, J.E., Patrick, D., Kihm, A.J., Foit Jr., F.F., Grandstaff, D.E., 2005. Lithostratigraphy, tephrochronology, and rare earth element geochemistry of fossils at the classical Pleistocene Fossil Lake area, South Central Oregon. J. Geol. 119, 139–155.

Masuda, A., Shimoda, J., Ikeuchi, Y., 1998. A depth coincidence between the lanthanide tetrad effect maximum and the oxic/anoxic interface at the Cariaco Trench off the Venezuelan coast. Geochem. J. 32, 275–280.

Meehan, T.J., 1994. Sediment analysis of the middle Whitney member: climatic implications for the upper Oligocene of western Nebraska. In: Dort Jr., W., (Ed.), TER-QUA Symp. Series 2. Institute for Tertiary-Quaternary Studies. Nebraska Acad. Sci., pp. 57–87.

Metzger, C., Terry Jr., D.O., Grandstaff, D.E., 2004. Effects of paleosol formation on rare earth element signatures in fossil bone. Geology 32, 497–500.

Miller, K.G., Fairbanks, R.G., Mountain, G.S., 1987. Tertiary oxygen isotope synthesis, sea level history, and continental margin erosion. Paleooceanog. 2, 1–19.

Mintz, J., Edelman, A., Terry Jr., D.O., Bright, R., 2005. Paleosols and vertebrate taphonomy of the Oligocene Poleslide member, Brule formation, Badlands National Park, South Dakota. Geol. Soc. Am. Abstr. with Prog. 37 (1), 13.

Monecke, T., Kempe, U., Monecke, J., 2003. Comment on the paper "W- and M-type tetrad effects in REE patterns for water–rock systems in the Tono uranium deposit, central Japan" by Y. Takahashi, H. Yoshida, N. Sato, K. Hama, Y. Yusa, and H. Shimizu. Chem. Geol. 202, 183–184.

Nesbitt, H.W., 1979. Mobility and fractionation of rare earth elements during weathering of a granodiorite. Nature 279, 206–210.

Nesbitt, H.W., Markovics, G., 1997. Weathering of granodioritic crust, long-term storage of elements in weathering profiles, and petrogenesis of siliclastic sediments. Geochim. Cosmochim. Acta 61, 1653–1670.

Obradovich, J.D., Evanoff, E., Larson, E.E., 1995. Revised single-crystal laser-fusion $^{40}Ar/^{39}Ar$ ages of Chadronian tuffs in the White River formation of Wyoming. Geol. Soc. Am. Abstr. with Prog. 27 (3), A-77.

Patrick, D., Martin, J.E., Parris, D.C., Grandstaff, D.E., 2004. Paleoenvironmental interpretations of rare earth element signatures in mosasaurs (Reptilia) from the upper Cretaceous Pierre Shale, Central South Dakota, USA. Palaeogeog. Palaeoecol. Palaeoclimatol. 212, 277–294.

Patrick, D., Martin, J.E., Parris, D.C., Grandstaff, D.E., 2007. Rare earth element determination of the stratigraphic position of the holotype of Mosasaurus missouriensis (Harlan), the first named fossil reptile from the American West. In: Martin, J.E., Parris, D.C. (Eds.), The Geology and Paleontology of the Late Cretaceous Marine Deposits of the Dakotas, vol. 427. Geol. Soc. Am. Spec. Paper, pp. 155–165.

Picard, S., Lecuyer, C., Barrat, J.A., Garcia, J.P., Dromart, G., Sheppard, S.M.F., 2002. Rare earth element contents of jurassic fish and reptile teeth and their potential relation to seawater composition (Anglo-Paris Basin, France and England). Chem. Geol. 186, 1–16.

Prothero, D.R., 1996. Magnetostratigraphy of the White River Group in the High Plains. In: Prothero, D.R., Emry, R.J. (Eds.), The Terrestrial Eocene–Oligocene Transition in North America. Cambridge University Press, New York, pp. 262–277.

Prothero, D.R., Whittlesey, K.E., 1998. Magnetic stratigraphy and biostratigraphy of the Orellan and Whitneyan Land mammal "Ages" in the White River Group. In: Terry, D.O., Jr., LaGarry, H.E., Hunt, R.M. (Eds.), Depositional Environments, Lithostratigraphy, and Biostratigraphy of the White River and Arikaree Groups (Late Eocene to Early Miocene, North America), vol. 325. Geol. Soc. Am. Spec. Paper, pp. 39–61.

Purnell, M.A., 2003. Casting, replication, and anaglyph stereo imaging of microscopic detail in fossils, with examplesfrom conodonts and other jawless vertebrates. Palaeontologia. Electronica 6, 11p.

Retallack, G.J., 1983. Late Eocene and Oligocene paleosols from Badlands National Park, South Dakota. Geol. Soc. Am. Spec.. Paper 193.

Rollinson, H.R., 1993. Using Geochemical Data: Evaluation, Presentation, Interpretation. Longman.

Schulz, M., Stattegger, K., 1997. SPECTRUM: Spectral analysis of unevenly spaced paleoclimatic time series. vol. 23. Computers Geosci., pp. 929–945. SPECTRUM available from: <http://www.geo.uni-bremen.de/geomod/staff/mschulz/#software>.

Shannon, R.D., Prewitt, C.T., 1969. Effective crystal radii in oxides and fluorides. Acta Crystallogr. Sect. B 25, 925–946.

Siegel, A.F., 1980. Testing for periodicity in a time series. J. Am. Stat. Assoc. 75, 345–348.

Spear, F.S., 1980. Plotting stereoscopic phase diagrams. Am. Mineral. 65, 1291–1293.

Staron, R.M., Grandstaff, B.S., Gallagher, W.B., Grandstaff, D.E., 2001. REE signatures in vertebrate fossils from Sewell, NJ; implications for location of the *K–T* boundary. PALAIOS 16, 255–265.

Suarez, C.A., Macpherson, G.L., Martin, L.D., Gonzlez, L.A., 2007a. Laser ablation ICP-MS analyses of fossil bone: preliminary results on rare earth element distribution in different types of fossil bone apatite. Geol. Soc. Am. Abstr. with Prog. 39, 18.

Suarez, C.A., Suarez, M.B., Terry Jr., D.O., Grandstaff, D.E., 2007b. Rare earth element geochemistry and taphonomy of the Early Cretaceous Crystal Geyser Dinosaur Quarry, east-central Utah. PALAIOS 22, 500–512.

Swisher, C.C., Prothero, D.R., 1990. Single crystal $^{40}Ar/^{39}Ar$ dating of the Eocene–Oligocene transition in North America. Science 249, 760–762.

Takahashi, Y., Yoshida, H., Sato, N., Harna, K., Yusa, Y., Shimizu, H., 2002. W- and M-type tetrad effects in REE patterns for water-rock systems in the Tono uranium deposit, central Japan. Chem. Geol. 184, 311–335.

Taylor, S.R., McLennen, S.M., 1985. The Continental Crust – Its Composition and Evolution. Blackwell Scientific Publication, Oxford, England.

Terry Jr., D.O., 1996. Stratigraphic and paleopedologic analysis of depositional sequences within the Pig Wallow site, Badlands National Park: National Park Service/University of Nebraska-Lincoln Cooperative Agreement #CA-1300-5-9001. Badlands National Park Archives.

Terry Jr., D.O., 1998. Lithostratigraphic revision and correlation of the lower part of the White River Group: South Dakota to Nebraska. In: Terry, D.O., Jr., LaGarry, H.E., Hunt, R.M. (Eds.), Depositional Environments, Lithostratigraphy, and Biostratigraphy of the White River and Arikaree Groups (Late Eocene to Early Miocene, North America), vol. 325. Geol. Soc. Am Spec. Paper, pp. 15–37.

Terry Jr., D.O., 2001. Paleopedology of the Chadron Formation of Northwestern Nebraska: implications for paleoclimate change in the North American mid-

continent across the Eocene–Oligocene boundary. Palaeogeog. Palaeoclimatol. Palaeoecol. 168, 1–38.

Terry Jr., D.O., LaGarry, H.E., 1998. Big Cottonwood Creek member: a new member of the Chadron Formation in North-Western Nebraska. In: Terry, D.O., Jr., LaGarry, H.E., Hunt, R.M. (Eds.), Depositional Environments, Lithostratigraphy, and Biostratigraphy of the White River and Arikaree Groups (Late Eocene to Early Miocene, North America), vol. 325. Geol. Soc. Am Spec. Paper, pp. 117–141.

Terry Jr., D.O., Spence, J.I., 1997. Documenting the extent and depositional environment of the Chadron Formation in the South Unit of Badlands National Park, National Park Service/University of Nebraska-Lincoln Cooperative Agreement #CA-1300-5-9001: Badlands National Park Archives. SD, USA.

Tiwari, R.K., 1987. Higher-order eccentricity cycles of the middle and late Miocene climatic variations. Nature 327, 219–221.

Trueman, C.N., 1999. Rare earth element geochemistry and taphonomy of terrestrial vertebrate assemblages. PALAIOS 14, 555–568.

Trueman, C.N., Behrensmeyer, A.K., Potts, R., Tuross, N., 2006. High-resolution records of location and stratigraphic provenance from the rare earth element composition in fossil bones. Geochim. Cosmochim. Acta 70, 4343–4355.

Trueman, C.N., Benton, M.J., 1997. A geochemical method to trace the taphonomic history of reworked bones in sedimentary settings. Geology 5, 263–266.

Trueman C. N., Tuross, N., 2002. Trace elements in recent and fossil bone apatite. In: Kohn, M.J., Rakovan, J., Hughes, J.M. (Eds), Phosphates: Geochemical, Geobiological, and Materials Importance. Reviews in Mineralogy and Geochemistry, vol. 48, pp. 489–521.

Trueman, C.N., Benton, M.J., Palmer, M.R., 2003. Geochemical taphonomy of shallow marine vertebrate assemblages. Palaeogeog. Palaeoclimatol. Palaeoecol. 197, 151–169.

Trueman, C.N.G., Field, J.H., Dortch, J., Charles, B., Wroe, S., 2005. Prolonged coexistence of humans and megafauna in Pleistocene Australia. Proc. US Natl. Acad. Sci. 102, 8381–8385.

Vondra, D.F., 1958. The stratigraphy of the Chadron Formation in northwestern Nebraska, M.S. Thesis. Univ. Nebraska, Lincoln, USA.

Walker, J.B., Choppin, G.R., 1967. Thermodynamic parameters of fluoride complexes of lanthanides. Adv. Chem. 71, 127–140.

Weedon, G.P., 2005. Time-Series Analysis and Cyclostratigraphy: Examining Stratigraphic Records of Environmental Cycles. Cambridge University Press, Cambridge.

Wood, S.A., 1990. The aqueous geochemistry of the rare-earth elements and yttrium. Review of available low-temperature data for inorganic complexes and the inorganic speciation of natural waters. Chem. Geol. 82, 159–186.

Wright, J., Schrader, H., Holser, W.T., 1987. Paleoredox variations in ancient oceans recorded by rare earth elements in fossil apatite. Geochim. Cosmochim. Acta 51, 631–644.

Zanazzi, A., Kohn, M.J., MacFadden, B.J., Terry Jr., D.O., 2007. Large temperature drop across the Eocene–Oligocene transition in central North America. Nature 445, 639–642.